Chemistry–A European Journal
Research Article
doi.org/10.1002/chem.202300898
Chemistry Europe
European Chemical Societies Publishing
www.chemeurj.org

Optimization and Automation of Helical Aromatic Oligoamide Foldamer Solid-Phase Synthesis

Valentina Corvaglia,[a] Florian Sanchez,[a] Friedericke S. Menke,[a] Céline Douat,[a] and Ivan Huc*[a]

Abstract: Helically folded oligoamides of 8-amino-2-quinolinecarboxylic acid composed of up to 41 units were prepared using optimized manual solid-phase synthesis (SPS). The high yield and purity of the final products places these SPS protocols among the most efficient known to date. Furthermore, analytical methods allowing for the clear identification and purity assessment of the products were validated, including ^{1}H NMR, a seldom used method for such large molecules. Adaption of the SPS protocols, in particular using in situ acid chloride activation under Appel's conditions, made it possible to efficiently implement SPS on a commercial peptide synthesizer, leading to a dramatic reduction of the laboratory work required to produce long sequences. Automation constitutes a breakthrough for the development of helical aromatic oligoamide foldamers.

Introduction

The advancement of efficient and reliable screening methodologies of peptides and peptide derivatives in the context of drug research such as, for example, display selection, has triggered a renewed interest for this class of compounds by the scientific community and pharmaceutical companies.[1] Concurrently, the offer in terms of peptide synthesis automation and parallelization has grown and new synthesizers have been launched on the market. Setting up a robust solid-phase peptide synthesis (SPPS) station is within the reach of many laboratories. In addition, recent achievements have unveiled the possibility to further accelerate the production of long peptides and entire proteins by relying on automated flow chemistry.[2] Along the same line, the level of perfection achieved in the solid-phase synthesis (SPS) of oligonucleotides using highly optimized variations of the phosphoramidite chemistry and fully automated synthesizers gives rapid and efficient access to all kinds of sequences.[3] The availability of synthetic oligonucleotides has enabled developments as diverse and important as PCR,[4] DNA-based nanotechnologies,[5] and therapeutic applications.[6]

In such a context of innovation, interest for efficient oligomer solid-phase synthetic methods has extended beyond peptides and nucleotides. For example, peptoids constitute a backbone with remarkable amenability to rapid SPS of long sequences (up to 36 units).[7] In the last decade, chemically diverse sequence-defined polymers produced by SPS have been designed and investigated for the purpose of information storage.[8] Conversely, foldamers are inherently oligomeric, and this field of research also requires its share of solid-phase synthetic methodologies (SPFS for solid-phase foldamer synthesis) to access to a variety of aliphatic[9] and aromatic[10] architectures and backbones in good purity and yield.

The efficiency of an SPS depends on multiple identified parameters that determine the yields of the many reaction steps carried out with no purification other than washing excess reagents away. However, not all these parameters are easy to control. The inherent efficacy of the chemical steps is of course central. For that reason, amide and phosphodiester formation, for which high yielding reactions are available, have been privileged. However, how these steps proceed also depends on the accessibility of the reactive functions on the resin to reagents in solution, which in turn depends on the conformations and possible aggregation of the sequences on the resin. Both aggregation and conformation may result into steric hindrance of coupling steps in a backbone-, length- and sequence-dependent manner. Optimizing the solvent, temperature, the nature of the resin and its swelling properties, or introducing specific removable chemical functions, may reduce on-resin aggregation or collapse of the growing sequences.[11] In practice, not many oligomer SPS show high conversion yields, i.e. good crude purity, beyond fifteen units. Poor purity may complicate final chromatographic purification though this may be partly alleviated by using capping reactions combined with capture and release approaches that prevent chain elongation after a failed coupling, and that may also confer distinct chromatographic retention behavior.[12]

[a] *Dr. V. Corvaglia, F. Sanchez, Dr. F. S. Menke, Dr. C. Douat, Prof. Dr. I. Huc*
Department of Pharmacy
Ludwig-Maximilians-Universität
Butenandtstr. 5–13, 81377 München (Germany)
E-mail: ivan.huc@cup.lmu.de
Homepage: https://huc.cup.uni-muenchen.de

Supporting information for this article is available on the WWW under https://doi.org/10.1002/chem.202300898

Several classes of aromatic oligoamides (AOs) have been produced by SPS, meeting the particular challenge of the lower reactivity of aromatic amines[10] as compared to peptidic aliphatic amines.[9] Among these, helical AOs stand out as a class of foldamers with stable and predictable conformations that result in useful properties for the purpose of, for example, exomolecular recognition of proteins,[13] tertiary folding design,[14] endomolecular recognition,[15] charge transport,[16] or to template peptide conformations in hybrid sequences.[17] In this context, various types of aromatic amino acid monomers have been designed and combined to promote helical folding. A common building block is 8-amino-2-quinolinecarboxylic acid Q (Figure 1). Q monomers may be decorated with various side chains in position 4, 5, or 6 that diverge from the folded oligomers.[18] Q_n helical conformations are very stable in apolar, polar aprotic and protic solvents.[19] Until now, denaturation conditions of these helices have not been identified and unfolded conformations could be populated only by means of mechanical force or interactions with a surface.[20]

The SPS of Q_n oligomers thus required overcoming the low nucleophilicity of 8-amino-quinolines and also the steric hindrance associated with helical folding that will occur as soon as three units have been assembled. In earlier reports, we introduced Q_n microwave-assisted manual SPFS using acid chloride activation.[10a,21] Here, we report developments of this methodology including its optimization to produce long sequences (>40 units, ≈9.8 kDa, in 70% crude yield) and its adaptation to automation thanks to the utilization of an in situ acid chloride activation based on Appel's reaction.[22] We also show the high amenability of long sequences to RP-HPLC purification and to ^{1}H NMR spectroscopic and mass spectrometry analysis. Altogether, our results place Q_n synthesis among the most robust and efficient SPS of non-peptidic non-nucleotidic sequences. We speculate that such efficiency may in fact result not despite, but thanks to, on-resin helical folding. These developments pave the way to the easy and fast production of new AOs sequences for the applications mentioned above.[13–17]

Results and Discussion

Manual SPFS, analysis and purification of a 15 mer

The previously published method for manual SPFS of Q_n oligomers has demonstrated its efficiency for sequences having over ten units.[18b,23] In order to benchmark the synthesis of longer oligomers and potential analysis or purification problems, we first investigated the preparation of 15mer **1** composed of hydrophobic (L), cationic (O) and anionic (D) residues (Figure 1). Because of the inherent curvature of Q_n helices – 2.5 units per turn – the two L residues of **1** are displayed on the same side of the helix (Figure 1c). The charged residues are placed without any particular order and ensure good water solubility. Sequences **2**–**4** are 14mers derived from the sequence of **1** by a single deletion. They could thus potentially arise as impurities of **1** when a coupling or preceding deprotection step would not be high yielding. Specifically, **2** misses the terminal cationic O unit of **1**, **3** misses a central O unit, and **4** misses an L unit. These different types of deletion were expected to result in variable changes in the RP-HPLC retention times (t_R) and ^{1}H NMR spectra of the 14mers.

All four sequences were prepared individually via SPFS on a 15 μmol scale. Starting from low loading brominated Wang resin (0.41 mmol/g), the immobilization of the first Fmoc-O(Boc)-OH monomer was carried out in the presence of CsI and DIEA.[10a] After standard Fmoc deprotection (DMF/piperidine), Fmoc-D(O*t*Bu)-OH was converted to its acid chloride with 1-chloro-*N*,*N*,2-trimethyl-1-propenyl-amine (Ghosez's reagent) and coupled to the amine of the first residue under microwave irradiation.[10a,21a] The following units were next assembled using the same deprotection/coupling cycles (Scheme 1). During SPFS, mini-cleavages of the resin-bound growing sequences were performed to validate intermediates and monitor the efficiency of the syntheses (see Supporting Information for details). Three full deprotection/coupling cycles require 4 h. If we consider the time needed to activate the acids into acid chlorides prior to SPFS, a busy work day of 8 h is filled (four

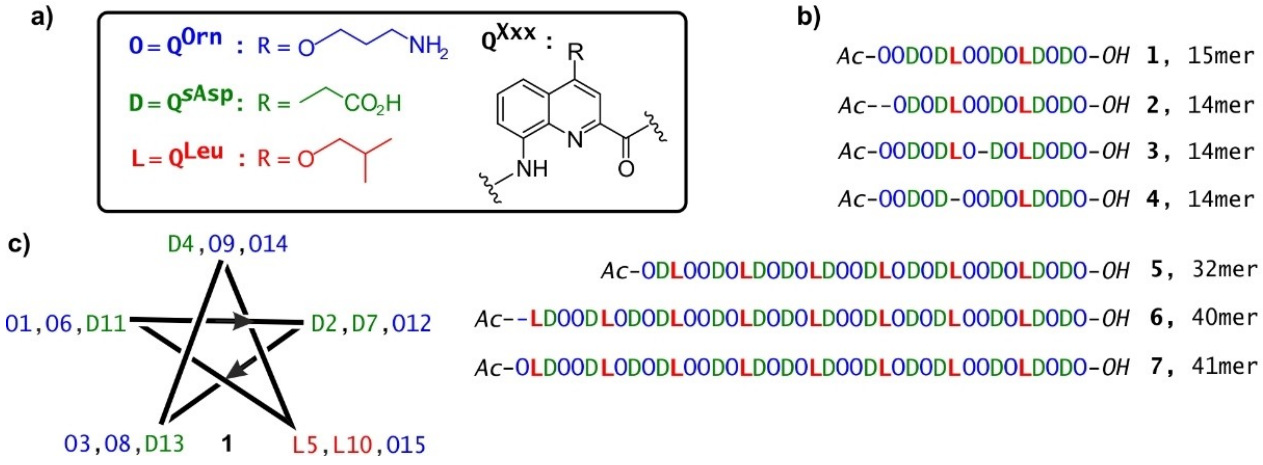

Figure 1. (a) Structures of quinoline monomers O, D and L (one letter code labels are inspired from those of α-amino acids). (b) Manually synthesized foldamer sequences. (c) Helical wheel projection of oligomer **1** showing the side-chain distribution along the 2.5 helix axis (5 aromatic units per two turns).

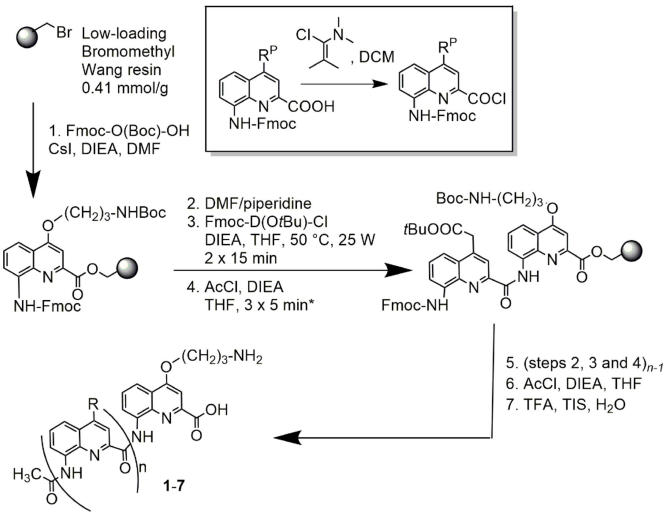

Scheme 1. SPFS protocols for oligomers **1**–**7**. R^P stands for protected R side-chain. *The acetylation capping step was introduced for sequences **5**–**7** only.

deprotection/coupling cycles are possible in a long work day of about 10 h). A 15mer such as **1** thus amounts to 40 h (5 work days), not counting the final deprotection and capping steps, and purification.

Foldamers **1**–**4** were finally N-acetylated prior to cleavage from the resin and side chain deprotection using a TFA/TIS/H_2O solvent mixture (95 : 2.5 : 2.5, v/v/v). Compounds **1**–**4** were then purified by RP-HPLC semi-preparative chromatography (isolated yields from 15–20% and purity > 99%). The purified chromatograms are shown in Figure 2a–d. The crude chromatogram of **1** is also shown in Figure 3a. Compounds were further characterized by ESI-MS and ^{1}H NMR (Figures 2f-g, S10, S11, S14, and S15). The chromatograms denote similar t_R values ascribable to the minor differences in sequence (Figure 2a–d). Nevertheless, upon optimizing RP-HPLC conditions with a shallow gradient, discrimination of the four different foldamers was achieved (Figure 2e). The retention times can be rationalized according to the hydrophilic/hydrophobic balance of the molecules. These chromatograms indicate that deleted products of a 15mer may be detected by RP-HPLC under optimized conditions but that preparative separation may become difficult. The mass spectra give clean charge envelopes that may allow for the detection of deleted sequences (Figure 2f). Differences were also clearly visible on ^{1}H NMR spectra where distinct chemical shifts of the amide NH signals were observed (Figure 2g). This level of discrimination for a single deletion contrasts with what may be expected with peptides of similar length.[24] If one deleted product was a contaminant of the 15mer, one could reasonably hope to detect it by NMR. In summary, the SPFS of a Q_{15} sequence proceeds smoothly and several reliable analytical methods of the final product purity are available. These results encouraged us to attempt the synthesis of even longer sequences.

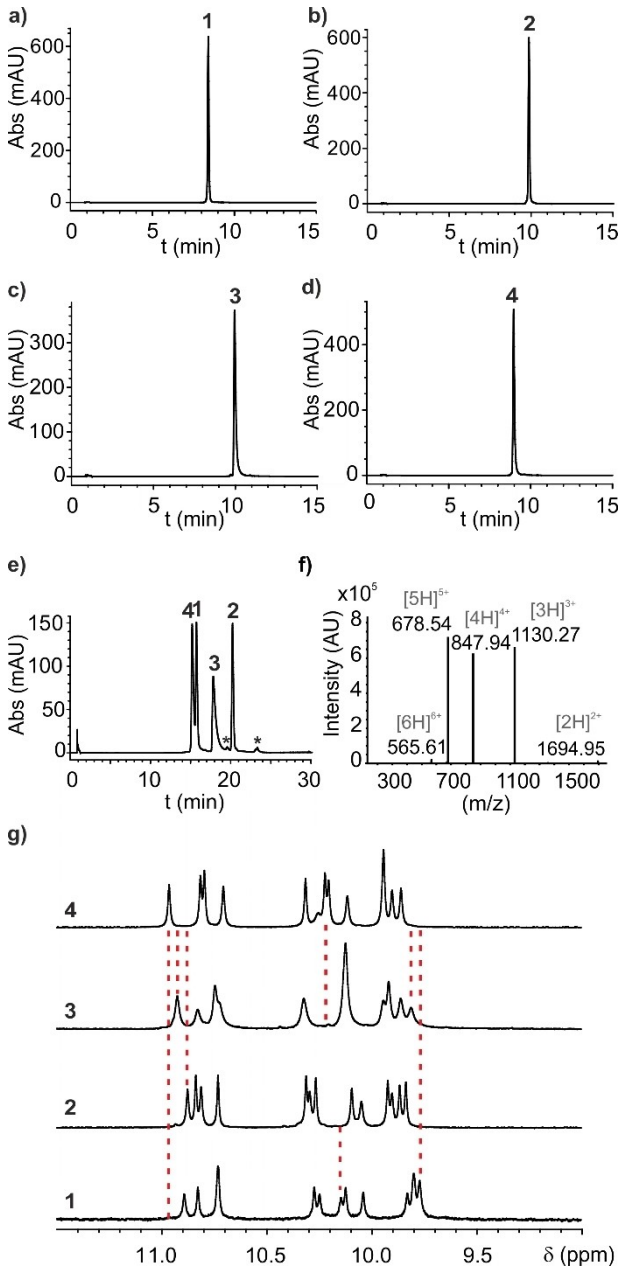

Figure 2. (a–d) RP-HPLC chromatograms of foldamers **1**–**4** using a linear gradient from 5% B to 40% B in 10 min; A: H_2O + 0.1% TFA and B: CH_3CN + 0.1% TFA. (e) RP-HPLC chromatogram of the co-injected foldamers **1**–**4** using a linear gradient from 5% B to 20% B in 23 min; A: H_2O, 0.1% TFA and B: CH_3CN 0.1% TFA. The stars show small impurities assigned to the solvents. (f) Representative example of multicharged species observed by ESI-MS of **1**. (g) NH amide region of the ^{1}H NMR spectra (700 MHz) of **1**–**4** (1 mM) in DMSO-d_6 at 60 °C. Red dashed lines indicate chemical shift (δ) differences between the NH amide resonances.

Manual SPFS, analysis and purification of a 41mer

In a second round of SPFS, oligoamides **5**–**7** were prepared (Figure 1). Sequence **5** is an extension of **2** to 32 units. Sequence **7** is an extension of **5** to 41 units. Sequence **6** is a 40mer missing the last unit of **7**. As for **1**–**4**, **5**–**7** have their hydrophobic L residues on the same face of the helix. Given the

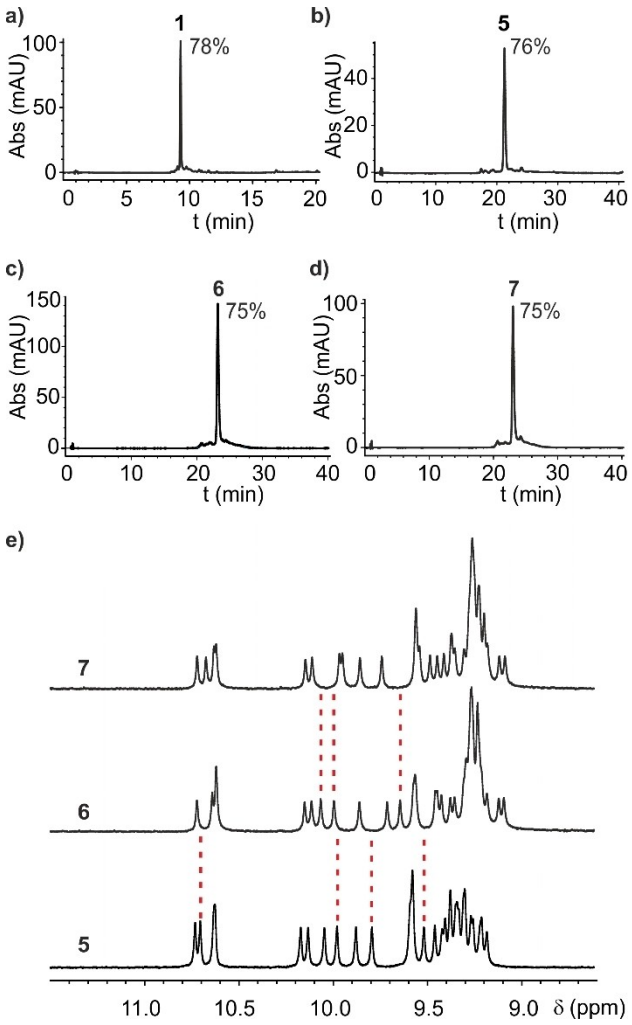

Figure 3. (a–d) RP-HPLC chromatograms of crude foldamers **1** introduced as a direct comparison, **5**, **6** and **7** showing the notable high purity obtained after **31**, **39** and **40** coupling cycles of SPFS (linear gradient from 20% B to 40% B in 35 min; A: H_2O + 0.1% TFA and B: CH_3CN + 0.1% TFA). (e) NH amide region of the ^{1}H NMR spectra (700 MHz) of **5**–**7** (1 mM) in DMSO-d_6 at 60 °C. Red dashed lines indicate the main chemical shift (δ) differences between the NH amide resonances.

similar t_R of **1**–**4** on RP-HPLC, it was expected that deleted products may be even more difficult to separate from the desired sequences in longer oligomers. Thus, a capping step was introduced after each coupling using acetyl chloride in the presence of DIEA in THF, at r.t. (3×5 min) as a modification of the SPFS procedure (step 4 in Scheme 1). Capping leads to truncated (instead of deleted) sequences that may be easier to separate, at least for the shorter ones. After TFA cleavage, the crude materials were analyzed by RP-HPLC (Figure 3b-3d). All chromatograms revealed one main product corresponding to the desired AO in high yield (over 70% after 40 SPS coupling cycles for **7**). The appearance of the crude chromatograms of **5**–**7** does not differ much from that of 15mer **1** (Figure 3a); thus demonstrating the robustness of the acid chloride-based SPFS methodology (Scheme 1). For comparison, Q_{41} is equivalent to an 82mer peptide in size. It appears that no drop in coupling and deprotection yields can be detected as elongation of the sequence is continued. This is all the more remarkable that the mass of foldamer exceeds the mass of resin at the end of the synthesis (for the 41mer, the mass of foldamer was three times bigger than the mass of resin). We hypothesize that on-resin helical folding during synthesis plays a favorable role. As shown in Figure 4a, the N-terminal amine function stacks on, and is sterically hindered by, the Q_n helix. However, this hindrance may also serve as a protection from further hindrance by other growing chains: the accessibility of the terminal amine would then not depend on the length of the neighboring chains. Furthermore, the fact that Q_n helices behave as rigid rods might favor their growth away from the resin and avoid the burial of a growing chain in the resin, which would result in a drop of coupling yield at some point (Figure 4b).

The purification of **5**–**7** was straightforward (isolated yields from 10–15% and purity >99% see Supporting Information). ESI-MS and ^{1}H NMR were again employed for the full characterization (Figures 3e, S12, S13, S16 and S17). As could be expected, even optimized RP-HPLC conditions did not allow for the separation of **6** and **7**. The chromatogram of a mixture of the two foldamers shows a single slightly broaden peak (Figure S9b). However, ^{1}H NMR spectroscopy allowed for the successful discrimination of these two compounds despite their minor difference in sequence (Figure 3e). Chemical shift values are different and ^{1}H NMR spectra would reveal the presence of **6** if it had been a significant inseparable impurity of **7**. The single set of sharp signals in the ^{1}H NMR spectrum of **7** is thus an excellent evidence of its high purity. ESI-MS also allows for efficient discrimination. By intentionally adding 10% of **6** to a solution of **7**, ESI-MS analysis reveal the presence of both foldamers. The absence of other ionized species in the mass spectra of **6** and **7** is also an indication of their purity (Figures S16b, S17).

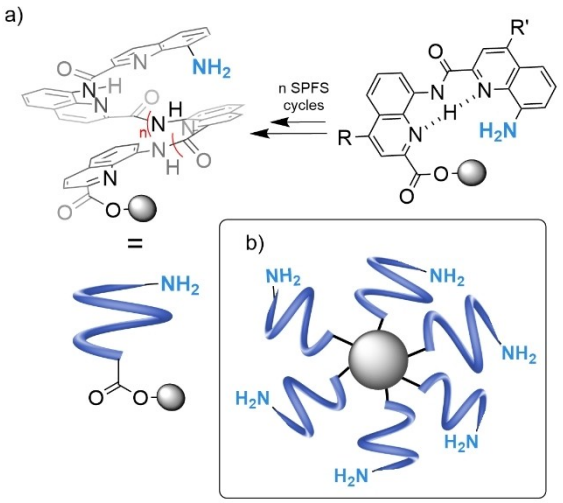

Figure 4. a) Schematic representation of a Q_n helix folding on a bead leaving the aromatic amine accessible for the next coupling. b) Cartoon depicting the hypothesis that on-bead foldamer sequences fold and grow away from the resin matrix.

In summary, sequences as long as a 41mer may be synthesized without any apparent drop in coupling efficiency or any particular difficulty in analyzing and purifying the product. We have probably reached the limit of resolution of our RP-HPLC C_{18} column for differentiating large foldamers with high sequence similarity, but ^{1}H NMR and ESI-MS remain efficient at detecting minor differences. Even longer sequences are probably within reach of our SPFS methodology but such syntheses face a practical inconvenience: they become overly labor intensive and time consuming. The synthesis of **7** amounted to 112 h (14 work days) not counting the final steps and purification. Rather than focusing on longer sequences, we considered the prospect of automating the synthesis.

Automated SPFS

From the beginning, we considered that SPFS automation entailed accessing acid chloride monomers without resorting to the Ghosez's reagent. In our hands, this reagent required a high vacuum evaporation of all solvent and unreacted reagent before subsequent coupling that would be difficult to implement on a synthesizer. Without complete evaporation, the Ghosez's reagent competes with the acid chloride to cap the amine of the growing chain. This eventually generates amidines that were identified by mass spectrometry and ^{1}H NMR (Scheme 2 and Figure S24). Wilson *et al.*, who used Ghosez's reagent in substoichiometric amounts with respect to the acid to be activated for aromatic amide SPFS apparently did not observe such side reactions with their monomers.[10b] They also pointed to the fact that this reaction may not be problematic, if it occurs, with secondary amines because the by-product would then be an unstable quaternary amidinium that could degrade back to the amine in the presence of a nucleophile. Thus, in situ coupling with Ghosez's reagent may be more robust in the case of secondary amines.[10b,c]

We have previously used Appel's reaction to activate α-amino acids as acid chlorides in situ, and couple them to Q monomers.[21b] We therefore opted for this method which allows for the addition of the acid chloride mixed with reagents and by- products involved in its formation directly onto the amine. A second issue was to find a commercial synthesizer amenable to a use quite different from its initial purpose. Automated SPPS is well-documented and standardized,[25] but implementing SPFS required significant adaptation for our purpose. We needed the synthesizer to enable: *i)* the formation of the acid chloride in a pre-activation vessel (PV) different from the reaction vessel (RV) containing the resin-bound foldamer; *ii)* an accurate and fast heating of RVs; *iii*) working under an inert nitrogen atmosphere; *iv)* high versatility in terms of solvent compatibility, including some solvents not friendly to many plastics and seals such as THF; and *v)* the optional parallel synthesis of several sequences. The following protocols have been optimized for the PurePep Chorus peptide synthesizer from Gyros-Protein Technology. This synthesizer met all the above-mentioned criteria. Other synthesizers may also work. However, protocols would then have to be adapted accordingly. For example, Wilson *et al.* premixed monomers with Ghosez's reagent in the amino acid delivery tube, allowing some sort of in situ activation without requiring a preactivation vessel.[10b,c]

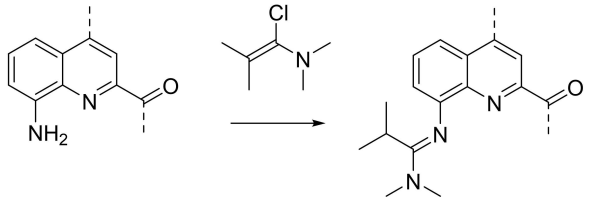

Scheme 2. Side reaction of 8-aminoquinolines with Ghosez's reagent producing an *N*,*N*-dimethyl-*N*′-(quinolin-8-yl)isobutyramidine.

An overview of the automated SPFS procedure is shown in Scheme 3. It entailed the programming of the synthesizer for the iteration of cycles consisting similar to those of manual SPFS (see Table S1 in the Supporting Information for detailed description): 1) Fmoc deprotection, 2) resin washings, 3) coupling, and 4) new round of washings. However, some changes were eventually implemented after several rounds of trials. We used low loading Cl-MPA ProTide resin (instead of the low loading Wang resin) because this resin has shown better purity of crude AOs during manual synthesis,[17a] and better AO recovery for sequences containing monomers bearing sulfonic acid side chains.[26] The Fmoc deprotection step was first tested using standard conditions (20% piperidine in DMF).

However, we noticed the occasional presence of a side product in the RP-HPLC chromatogram of the crude AOs when using piperidine. This side product never occurred during manual synthesis. LC-MS analysis of the side product indicated +67 Da in mass with respect to the target mass. This corresponds to the addition of a piperidine molecule on the foldamer together with the loss of a water molecule. A possible side reaction may be the formation of a piperidinoaminidine that might arise from the activation of an amide into an imidoyl chloride by the in situ coupling reagents.[27] However, this hypothesis has not been ascertained. Nevertheless, the piperidine-derived adduct never formed when removing Fmoc protecting groups using 2% DBU in NMP, so we opted for these conditions instead. Using DBU also proved more efficient than piperidine for monomers other than those discussed in this study and which will be described elsewhere.

Preactivation of the acid into the acid chloride was implemented in the PV by successive additions of the Fmoc-Q-OH monomer (3 equiv. relative to resin loading), Ph_3P (8 equiv.) and trichloroacetonitrile (TCAN, 9 equiv.) solutions in anhydrous THF and shaking the PV for 1 min before dispensing the acid chloride solution from the PV to the RV containing the resin pre-swollen with a solution of 2,4,6-collidine (9 equiv.) in anhydrous THF (Scheme 3). The acid chloride is formed in the absence of base using dry THF and reagents (moisture would lead to the production of HCl that would alter acid labile protecting groups of the side chains). Other solvents than THF can be used when needed. For example, NMP/THF (1:1 v/v) was used to solubilize Fmoc-O(Boc)-OH. Yet THF is preferable

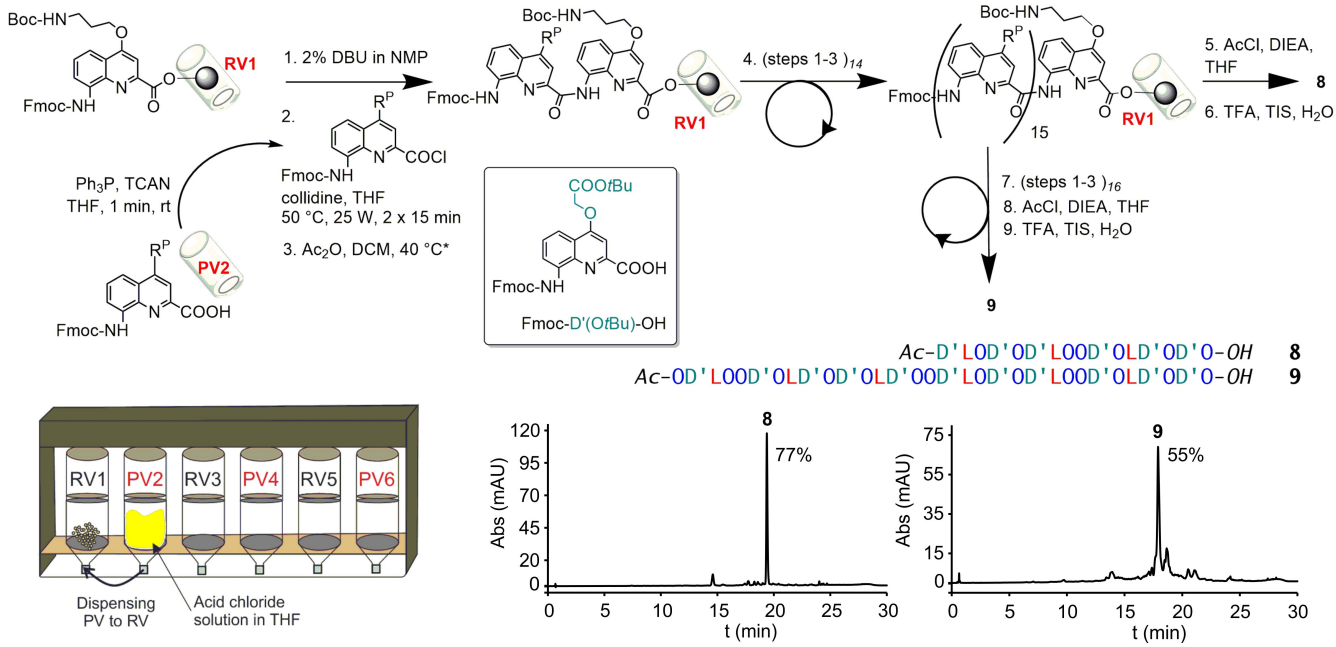

Scheme 3. SPFS protocols developed for the automation of the AO synthesis and exemplified for 16mer **8** and 32mer **9**. Bottom left: schematic representation of the Chorus synthesizer with RVs and PVs used during the coupling cycles. *The capping step was introduced after the 8th coupling. Bottom right: RP-HPLC chromatograms of foldamers **8** and **9** (linear gradient from 20% B to 40% B in 23 min; A: H_2O + 0.1% TFA and B: CH_3CN + 0.1% TFA).

for reasons that are detailed in the next section. The RV was next heated to 50 °C for 15 min before draining and resin washings with anhydrous THF. The coupling reaction was repeated once. Capping with acetic anhydride in DCM (50:50, v/v) at 40 °C for 10 min may be implemented prior to the next deprotection.[28]

The syntheses of 16mer **8** and of 32mer **9** are presented as representative examples of automated SPFS (Scheme 3). The sequence of **9** is identical to that of **5** but D units were replaced by the related D′ (Fmoc-D′(O*t*Bu)-OH as shown in Scheme 3). D′ is intensively used in our group and stocks are generally available. It is also easier and cheaper to produce than D. Sequence **8** corresponds to the sixteen C-terminal units of **9**. The syntheses were performed on a 15 μmol scale starting with the C-terminal Fmoc-O(Boc) preloaded on the MPA-Protide resin in 10 mL glass RVs (Scheme 3). This scale is the smallest for which we obtained good results. Scaling up the SPFS on the Chorus synthesizer can be implemented without hurdles. Three different RV sizes are available (10, 25, 40 mL) and allow to work at a scale up to 500 μmol. During the syntheses, a capping step was introduced after the 8th coupling. After final Fmoc deprotection and acetylation, **8** and **9** were cleaved from the resin and their purity was checked by RP-HPLC analysis. Sequence **8** was recovered in very good amount (50 mg of crude out of 59 mg expected, 85%). The RP-HPLC chromatogram showed one main peak indicating a crude purity of 77% (Scheme 3). Product identity was established by LC-MS analysis (Figure S18a). In terms of purity and amount recovered, these values are comparable to those obtained for the manual SPFS of **1**. The main difference between the two approaches is the significant reduction of work time. The automated SPFS of **8** required 2–3 h of work to prepare solutions followed by 19 h of instrument time, in comparison to 40 h of work (5 work days) required for the manual SPFS of **1**. Results were also satisfactory for the preparation of 32mer **9** whose identity was confirmed by LC-MS analysis (Figure S18b). The mass recovered was 83% of that expected. The RP-HPLC analysis showed a drop of crude purity with respect to manually synthesized **7** (55% versus 77%). This suggests that the couplings using the Appel reaction may not perform as perfectly as the activation with the Ghosez's reagent which may be understood given the complexity of the Appel reaction as discussed in the next section. Nevertheless, these yields compare favorably to the SPS of peptides of similar length (Q_{32} is equivalent to 64 α-amino acids, i.e. protein size).[29] The critical point is again the time saved. The preparation of **9** also required 2–3 h of work to set-up the Chorus synthesizer followed by 40 h of non-stop instrument time, to be compared to 88 h (11 work days) for the manual synthesis of **5**.

Monomer recycling

The automation of large AO SPFS plus the possibility to build up to three sequences in parallel makes the availability of monomers a limiting factor. Suitably protected Q monomers all require a multistep synthesis for their preparation. Even if these syntheses have been streamlined on a multigram scale, the monomers are valuable and used in excess (2×3 equiv.) during SPFS. We were therefore motivated to implement monomer recovery. The basic coupling reaction mixture that flows from the RV after coupling can be quenched by collecting it in a 5%

aqueous citric acid solution. This can be easily implemented by inserting a collect step in the protocol which will dispense the coupling solution to the collect container. The citric acid serves to protonate the acid function of Fmoc-Q-OH, thus allowing its subsequent extraction in CH_2Cl_2, without damaging acid labile side chain protections. The extracted mixtures, however, may be more complicated than expected. RP-HPLC analysis allowed us to assess the presence of other substances than the Fmoc-Q-OH to be recycled. The most typical, and potentially most abundant species is a stable ylide. In the case of monomer L, this ylide was purified and characterized and its structure was confirmed by LC-MS, ^{1}H NMR, and x-ray crystallography (compound **10** in Scheme 4, Figure S19 and Table S3). Compound **10** results from the reaction of the acid chloride with (cyanomethylene)-triphenylphosphorane **11** ($Ph_3P{=}CH_2CN$).[30] This reaction

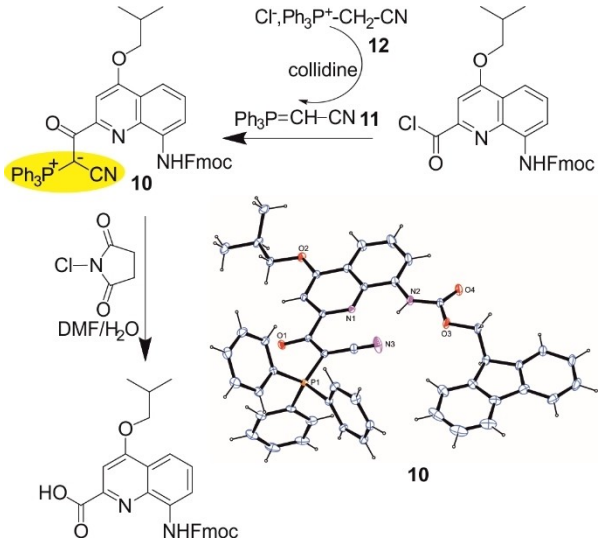

Scheme 4. Formation and crystal structure of ylide **10** produced during in situ acid chloride activation using TCAN, Ph_3P and Fmoc-L-OH monomer.

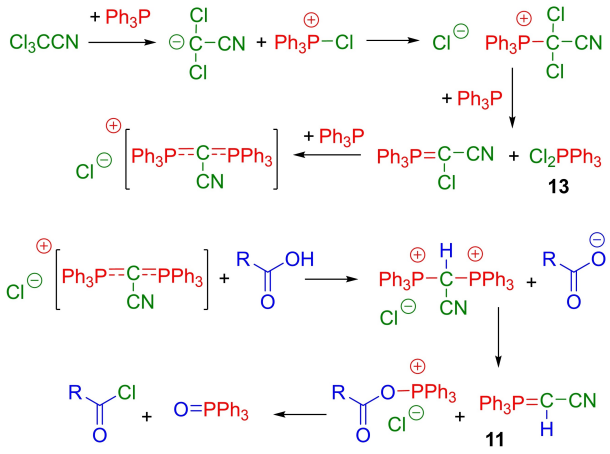

Scheme 5. Mechanism of the TCA/triphenylphosphine-mediated activation of an acid into an acid chloride explaining the formation of **11** as a by-product, adapted from Ref. [22a] where CCl_4 was used instead of TCAN. The colors of atoms belonging to the reagents are reflected in the formulas of the products.

could indeed be reproduced using commercial **11** (Figure S20). The presence of **11** in the reaction mixture is consistent with Appel's report that (chloromethylene)-triphenylphosphorane forms when using CCl_4 instead of TCAN (Eq. (57) in Ref. [22a]). The mechanism that leads to the formation of **11** is depicted in Scheme 5. The presence of **11** in the activation step thus threatens to reduce the amount of available acid chloride. However, when activation is performed in THF, we observe that (cyanomethyl)triphenylphosphonium chloride **12** (Scheme 4) immediately precipitates and remains in the PV after the acid chloride solution has been transferred to the RV. Collecting a sample of the precipitate allowed us to assign it to pure **12** (Figure S21). Subsequent washing of the PV with DMF flushes this precipitate away. A benefit of using THF for the activation step is thus to reduce the formation of ylides such as **10**. The proportion of ylide is for example higher for Fmoc-O(Boc)-OH which is activated in THF/NMP from which **12** does not precipitate.

Of note, the mechanism shown in Scheme 5 is typical of an acid chloride activation under neutral conditions: it does not generate HCl unlike many other typical reagents (e.g. $SOCl_2$, oxalyl chloride). However, this mechanism accounts for the formation of **11**, but not of the salt **12** which we isolated. A possible explanation for the presence of **12** may be the dichlorotriphenylphosphorane **13** that is generated during the activation. Compound **13** may also react with the carboxylic acid to produce the acid chloride, triphenylphosphine oxide and HCl. HCl would then be buffered by **11** to produce **12**. Another possible, less desirable, source of HCl is the reaction of the acid chloride with **11**. Indeed, when reacting Fmoc-L–Cl with **11**, **10** is produced along with **12**, showing the ability of **11** to act as a base and as a nucleophile (Figure S20). Of note, HCl is anyways produced during the subsequent coupling step, regardless of the pathway that produces the acid chloride, but the coupling is always performed in presence of a base.

Ylides such as by-product **10** are stable.[30] Yet we found that it is possible to chlorinate them with *N*-chlorosuccinimide (NCS) leading to their degradation into a carboxylic acid (Scheme 4), through a haloform-like reaction similar to the degradation of cyanosulfurylides recently developed as selective protecting group of Asp residue during SPPS.[31] Thus, **10** was exposed to increasing amounts of NCS in a DMF/H_2O mixture. The reaction was monitored by RP-HPLC analysis and proved to be almost complete after 2 days using up to 5 equivalents of NCS (Figure S22). In summary, excess Fmoc-protected monomers may be recycled after quenching the coupling reaction mixtures. In case significant amounts of cyanoketophosphoranes are present, these may be degraded back to the desired acid using NCS, before final purification.

Consequences for manual synthesis

The adaptation and optimization of the protocols for the automation of SPFS have led to developments that can also be useful in manual synthesis. For instance, the in situ activation via the Appel's reaction is much quicker to implement than the

activation with Ghosez's reagent, allowing five deprotection/coupling cycles to be performed manually in 8–9 h. For this, we used the same reagents and the same stoichiometry with respect to Fmoc-Q-OH as for the automated synthesis. In manual synthesis, the acid activation mixture is typically transferred unfiltered to the resin. This requires a better solvent than pure THF and $CHCl_3$/THF (1:1, v/v) was typically used to dissolve all intermediates (including **12**). Acid chloride activation is then performed in a separate vial shaken by hand for a few seconds before being added to the resin suspended in THF containing collidine. Consequently, one has to anticipate the potential presence of ylide by-products when recovering the Fmoc-Q-OH after a manual coupling cycle. Other coupling cycle optimizations are currently being tested, including the reduction of the number of equivalents of Fmoc-Q-OH monomer and of activating reagents, or of the time necessary for complete Fmoc deprotection with 2% DBU in NMP. Progress will be reported in due course.

Conclusion

We have extended the manual SPS and the analysis and purification of helically folded aromatic oligoamides to sequences as long as a 41mer with excellent yields and purity. This places our SPS protocols among the most efficient known to date, giving access to sequences in the size range of an 80mer peptide. We speculate that this remarkable efficiency is in fact assisted by helical folding on the resin. This would contrast with the common observation in peptide synthesis that on-resin folding and aggregation result in decreasing coupling yields. Next, we have adapted and optimized the deprotection and coupling procedures to allow for the automation of the SPFS. A commercial peptide synthesizer was used to produce aromatic oligoamide sequences starting from Fmoc-acid monomers, that is, including their activation to acid chlorides in a preactivation vessel under a nitrogen atmosphere. Long AO sequences were produced with minimal laboratory work in good (32mer **9**) to high (16mer **8**) crude purity. The validation of the analytical techniques (RP-HPLC, NMR, and LC-ESI-MS) allowed for the identification and full characterization of the designed foldamers. This is of special importance for long and more complex structures, usually designed for biological or biomaterial applications, for which the final step of analysis and purification can be a limitation. These developments pave the way to the rapid access to new and longer sequences than before, and thus to quicker exploration of their properties. Automated SPFS of multiple sequences will also permit to investigate the ligation of long, pre-synthesized, fragments, as in protein synthesis, and to potentially explore the behavior of foldamers of 10 kDa and above.

Supporting Information

The data that support the findings of this study are available in the supplementary material of this article. Additional references cited within the Supporting Information.[32–35]

Deposition Number(s) 2243294 (for **10**) contain(s) the supplementary crystallographic data for this paper. These data are provided free of charge by the joint Cambridge Crystallographic Data Centre and Fachinformationszentrum Karlsruhe Access Structures service.

Acknowledgements

We are grateful to the Deutsche Forschungsgemeinschaft (DFG) for financial support via project HU1766/2-1 and CRC1309-C7 (project ID 325871075). We thank Dr. D. Bindl for helping with monomer recovery procedures, Dr. P. Mayer for assistance with crystallographic measurements and structure elucidation, and I. R. Alonso for the isolation and characterization of the *N*,*N*-dimethyl-*N*′-(quinolin-8-yl)isobutyramidine. Open Access funding enabled and organized by Projekt DEAL.

Conflict of Interests

The authors declare no conflict of interest.

Data Availability Statement

The data supporting these findings are available upon reasonable request from the authors. Deposition Number 2243294 (for **10**) contains the supplementary crystallographic data for this paper. These data are provided free of charge by the joint Cambridge Crystallographic Data Centre and Fachinformationszentrum Karlsruhe Access Structures service.

Keywords: aromatic oligoamides · automation · foldamers · in situ acid chloride activation · solid-phase synthesis

[1] a) L. Wang, N. Wang, W. Zhang, X. Cheng, Z. Yan, G. Shao, X. Wang, R. Wang, C. Fu, *Signal Transduct. Target. Ther.* **2022**, *7*, 48; b) C. Heinis, T. Rutherford, S. Freund, G. Winter, *Nat. Chem. Biol.* **2009**, *5*, 502–507; c) B. He, K. F. Tjhung, N. J. Bennett, Y. Chou, A. Rau, J. Huang, R. Derda, *Sci. Rep.* **2018**, *8*, 1214; d) J. Y. K. Wong, R. Mukherjee, J. Miao, O. Bilyk, V. Triana, M. Miskolzie, A. Henninot, J. J. Dwyer, S. Kharchenko, A. Iampolska, D. M. Volochnyuk, Y.-S. Lin, L.-M. Postovit, R. Derda, *Chem. Sci.* **2021**, *12*, 9694–9703; e) T. R. Oppewal, I. D. Jansen, J. Hekelaar, C. Mayer, *J. Am. Chem. Soc.* **2022**, *144*, 3644–3652; f) T. Passioura, T. Katoh, Y. Goto, H. Suga, *Annu. Rev. Biochem.* **2014**, *83*, 727–752; g) W. Liu, S. J. de Veer, Y.-H. Huang, T. Sengoku, C. Okada, K. Ogata, C. N. Zdenek, B. G. Fry, J. E. Swedberg, T. Passioura, D. J. Craik, H. Suga, *J. Am. Chem. Soc.* **2021**, *143*, 18481–18489.

[2] a) N. Hartrampf, A. Saebi, M. Poskus, Z. P. Gates, A. J. Callahan, A. E. Cowfer, S. Hanna, S. Antilla, C. K. Schissel, A. J. Quartararo, X. Ye, A. J. Mijalis, M. D. Simon, A. Loas, S. Liu, C. Jessen, T. E. Nielsen, B. L. Pentelute, *Science* **2020**, *368*, 980–987; b) H. Masui, S. Fuse, *Org. Process Res. Dev.* **2022**, *26*, 1751–1765; c) M. D. Simon, P. L. Heider, A. Adamo, A. A. Vinogradov, S. K. Mong, X. Li, T. Berger, R. L. Policarpo, C. Zhang, Y.

Zou, X. Liao, A. M. Spokoyny, K. F. Jensen, B. L. Pentelute, *ChemBioChem* **2014**, *15*, 713–720.
[3] a) I. Sarac, C. Meier, *Chem. Eur. J.* **2015**, *21*, 16421–16426; b) D. A. Lashkari, S. P. Hunicke-Smith, R. M. Norgren, R. W. Davis, T. Brennan, *Proc. Natl. Acad. Sci. USA* **1995**, *92*, 7912–7915; c) S. Pitsch, P. A. Weiss, X. Wu, D. Ackermann, T. Honegger, *Helv. Chim. Acta* **1999**, *82*, 1753–1761; d) M. D. Matteucci, M. H. Caruthers, *J. Am. Chem. Soc.* **1981**, *103*, 3185–3191; e) S. Roy, M. Caruthers, *Molecules* **2013**, *18*, 14268–14284; f) A. F. Sandahl, T. J. D. Nguyen, R. A. Hansen, M. B. Johansen, T. Skrydstrup, K. V. Gothelf, *Nat. Commun.* **2021**, *12*, 2760.
[4] D. M. Hoover, J. Lubkowski, *Nucleic Acids Res.* **2002**, *30*, e43.
[5] N. C. Seeman, *Trends Biotechnol.* **1999**, *17*, 437–443.
[6] D. D. Ma, T. Rede, N. A. Naqvi, P. D. Cook, *Biotechnol. Annu. Rev.* **2000**, *5*, 155–196.
[7] H. Tran, S. L. Gael, M. D. Connolly, R. N. Zuckermann, *J. Visualization* **2011**, *57*, e3373.
[8] a) K. R. Strom, J. W. Szostak, *J. Org. Chem.* **2020**, *85*, 13929–13938; b) R. K. Roy, A. Meszynska, C. Laure, L. Charles, C. Verchin, J.-F. Lutz, *Nat. Commun.* **2015**, *6*, 7237.
[9] a) J. K. Murray, S. H. Gellman, *Org. Lett.* **2005**, *7*, 1517–1520; b) C. Douat-Casassus, K. Pulka, P. Claudon, G. Guichard, *Org. Lett.* **2012**, *14*, 3130–3133; c) A. Abdildinova, M. J. Kurth, Y.-D. Gong, *Asian J. Org. Chem.* **2021**, *10*, 2300–2317.
[10] a) B. Baptiste, C. Douat-Casassus, K. Laxmi-Reddy, F. Godde, I. Huc, *J. Org. Chem.* **2010**, *75*, 7175–7185; b) N. S. Murphy, P. Prabhakaran, V. Azzarito, J. P. Plante, M. J. Hardie, C. A. Kilner, S. L. Warriner, A. J. Wilson, *Chem. Eur. J.* **2013**, *19*, 5546–5550; c) K. Long, T. A. Edwards, A. J. Wilson, *Bioorg. Med. Chem.* **2013**, *21*, 4034–4040; d) H. M. König, R. Abbel, D. Schollmeyer, A. F. Kilbinger, *Org. Lett.* **2006**, *8*, 1819–1822; e) E. E. Baird, P. B. Dervan, *J. Am. Chem. Soc.* **1996**, *118*, 6141–6146.
[11] a) M. Badoux, A. F. M. Kilbinger, *Macromolecules* **2017**, *50*, 4188–4197; b) L. K. Mueller, A. C. Baumruck, H. Zhdanova, A. A. Tietze, *Front. Bioeng. Biotechnol.* **2020**, *8*, 162.
[12] V. Aucagne, I. E. Valverde, P. Marceau, M. Galibert, N. Dendane, A. F. Delmas, *Angew. Chem. Int. Ed.* **2012**, *51*, 11320–11324; *Angew. Chem.* **2012**, *124*, 11482–11486.
[13] a) K. Ziach, C. Chollet, V. Parissi, P. Prabhakaran, M. Marchivie, V. Corvaglia, P. P. Bose, K. Laxmi-Reddy, F. Godde, J.-M. Schmitter, S. Chaignepain, P. Pourquier, I. Huc, *Nat. Chem.* **2018**, *10*, 511–518; b) V. Corvaglia, D. Carbajo, P. Prabhakaran, K. Ziach, P. K. Mandal, V. D. Santos, C. Legeay, R. Vogel, V. Parissi, P. Pourquier, I. Huc, *Nucleic Acids Res.* **2019**, *47*, 5511–5521; c) J. Ahmed, T. C. Fitch, C. M. Donnelly, J. A. Joseph, T. D. Ball, M. M. Bassil, A. Son, C. Zhang, A. Ledreux, S. Horowitz, Y. Qin, D. Paredes, S. Kumar, *Nat. Commun.* **2022**, *13*, 2273; d) S. Kumar, M. Birol, D. E. Schlamadinger, S. P. Wojcik, E. Rhoades, A. D. Miranker, *Nat. Commun.* **2016**, *7*, 11412; e) D. Maity, S. Kumar, F. Curreli, A. K. Debnath, A. D. Hamilton, *Chem. Eur. J.* **2019**, *25*, 7265–7269.
[14] S. De, B. Chi, T. Granier, T. Qi, V. Maurizot, I. Huc, *Nat. Chem.* **2018**, *10*, 51–57.
[15] a) Y. Ferrand, I. Huc, *Acc. Chem. Res.* **2018**, *51*, 970–977; b) V. Koehler, A. Roy, I. Huc, Y. Ferrand, *Acc. Chem. Res.* **2022**, *55*, 1074–1085; c) T. A. Sobiech, Y. Zhong, B. Gong, *Org. Biomol. Chem.* **2022**, *20*, 6962–6978; d) T. A. Sobiech, Y. Zhong, D. P. Miller, J. K. McGrath, C. T. Scalzo, M. C. Redington, E. Zurek, B. Gong, *Angew. Chem. Int. Ed.* **2022**, *61*, e202213467; *Angew. Chem.* **2022**, *134*, e202213467; e) J.-L. Hou, X.-B. Shao, G.-J. Chen, Y.-X. Zhou, X.-K. Jiang, Z.-T. Li, *J. Am. Chem. Soc.* **2004**, *126*, 12386–12394; f) C. Li, S.-F. Ren, J.-L. Hou, H.-P. Yi, S.-Z. Zhu, X.-K. Jiang, Z.-T. Li, *Angew. Chem. Int. Ed.* **2005**, *44*, 5725–5729; *Angew. Chem.* **2005**, *117*, 5871–5875.
[16] X. Li, N. Markandeya, G. Jonusauskas, N. D. McClenaghan, V. Maurizot, S. A. Denisov, I. Huc, *J. Am. Chem. Soc.* **2016**, *138*, 13568–13578.
[17] a) S. Dengler, P. K. Mandal, L. Allmendinger, C. Douat, I. Huc, *Chem. Sci.* **2021**, *12*, 11004–11012; b) S. Dengler, C. Douat, I. Huc, *Angew. Chem. Int. Ed.* **2022**, *61*, e202211138; *Angew. Chem.* **2022**, *134*, e202211138.
[18] a) X. Hu, S. J. Dawson, P. K. Mandal, X. de Hatten, B. Baptiste, I. Huc, *Chem. Sci.* **2017**, *8*, 3741–3749; b) M. Zwillinger, P. S. Reddy, B. Wicher, P. K. Mandal, M. Csékei, L. Fischer, A. Kotschy, I. Huc, *Chem. Eur. J.* **2020**, *26*, 17366–17370.
[19] T. Qi, V. Maurizot, H. Noguchi, T. Charoenraks, B. Kauffmann, M. Takafuji, H. Ihara, I. Huc, *Chem. Commun.* **2012**, *48*, 6337–6339.
[20] a) F. Devaux, X. Li, D. Sluysmans, V. Maurizot, E. Bakalis, F. Zerbetto, I. Huc, A.-S. Duwez, *Chem* **2021**, *7*, 1333–1346; b) D. Meier, B. Schoof, J. Wang, X. Li, A. Walz, A. Huettig, H. Schlichting, F. Rosu, V. Gabelica, V. Maurizot, J. Reichert, A. C. Papageorgiou, I. Huc, J. V. Barth, *Chem. Commun.* **2022**, *58*, 8938–8941.
[21] a) S. J. Dawson, X. Hu, S. Claerhout, I. Huc, in *Methods Enzymol.*, Vol. 580 (Ed.: V. L. Pecoraro), Academic Press, Cambridge, Massachusetts, United States, **2016**, Ch. 13; b) X. Hu, S. J. Dawson, Y. Nagaoka, A. Tanatani, I. Huc, *J. Org. Chem.* **2016**, *81*, 1137–1150.
[22] a) R. Appel, *Angew. Chem. Int. Ed. Engl.* **1975**, *14*, 801–811; *Angew. Chem.* **1975**, *24*, 863–874; b) D. O. Jang, D. J. Park, J. Kim, *Tetrahedron Lett.* **1999**, *40*, 5323–5326; c) L. E. Barstow, V. J. Hruby, *J. Org. Chem.* **1971**, *36*, 1305–1306.
[23] a) P. S. Reddy, B. Langlois d'Estaintot, T. Granier, C. D. Mackereth, L. Fischer, I. Huc, *Chem. Eur. J.* **2019**, *25*, 11042–11047; b) F. S. Menke, B. Wicher, V. Maurizot, I. Huc, *Angew. Chem. Int. Ed.* **2023**, *62*, e202217325; *Angew. Chem.* **2023**, *135*, e202217325.
[24] For peptides of similar length, NMR spectra are poorly informative about compound identity or purity so much so that they are generally not requested for publication in organic chemistry journals.
[25] a) J. Tian, Y. Li, B. Ma, Z. Tan, S. Shang, *Front. Chem.* **2022**, *10*, 896098; b) F. Zieleniewski, D. N. Woolfson, J. Clayden, *Chem. Commun.* **2020**, *56*, 12049–12052; c) Y. Yu, A. Kononov, M. Delbianco, P. H. Seeberger, *Chem. Eur. J.* **2018**, *24*, 6075–6078; d) D. F. H. Winkler, in *Peptide Synthesis: Methods and Protocols*, Vol. 2103 (Eds.: W. M. Hussein, M. Skwarczynski, I. Toth), Springer US, New York, United States, **2020**.
[26] D. Bindl, P. K. Mandal, L. Allmendinger, I. Huc, *Angew. Chem. Int. Ed.* **2022**, *61*, e202116509; *Angew. Chem.* **2022**, *134*, e202116509.
[27] a) E. A. O'Brien, K. K. Sharma, J. Byerly-Duke, L. A. Camacho, III, B. VanVeller, *J. Am. Chem. Soc.* **2022**, *144*, 22397–22402; b) D. M. Szantai-Kis, C. R. Walters, T. M. Barrett, E. M. Hoang, E. J. Petersson, *Synlett* **2017**, *28*, 1789–1794.
[28] Ac_2O was preferred for the capping step. We avoided to introduce AcCl, which is highly reactive and potentially corrosive, in the synthesizer. Ac_2O had previously been shown to be efficient for this purpose (see Ref. [10a]).
[29] a) M. Cemazar, D. J. Craik, *J. Pept. Sci.* **2008**, *14*, 683–689; b) R. D. M. Silva, J. Franco Machado, K. Gonçalves, F. M. Lucas, S. Batista, R. Melo, T. S. Morais, J. D. G. Correia, *Molecules* **2021**, *26*, 7349.
[30] H. H. Wasserman, W.-B. Ho, *J. Org. Chem.* **1994**, *59*, 4364–4366.
[31] K. Neumann, J. Farnung, S. Baldauf, J. W. Bode, *Nat. Commun.* **2020**, *11*, 982.
[32] Bruker (**2012**). SAINT. Bruker AXS Inc., Madison, Wisconsin, USA.
[33] G. M. Sheldrick (**1996**). SADABS. University of Göttingen, Germany.
[34] G. M. Sheldrick, *Acta Crystallogr. Sect. A* **2015**, *71*, 3–8.
[35] A. L. Spek, *Acta Crystallogr. Sect. C* **2015**, *71*, 9–18.

Manuscript received: March 21, 2023
Accepted manuscript online: April 6, 2023
Version of record online: May 5, 2023